

Journal of Materials Chemistry A

Accepted Manuscript



This is an *Accepted Manuscript*, which has been through the Royal Society of Chemistry peer review process and has been accepted for publication.

Accepted Manuscripts are published online shortly after acceptance, before technical editing, formatting and proof reading. Using this free service, authors can make their results available to the community, in citable form, before we publish the edited article. We will replace this *Accepted Manuscript* with the edited and formatted *Advance Article* as soon as it is available.

You can find more information about *Accepted Manuscripts* in the [Information for Authors](#).

Please note that technical editing may introduce minor changes to the text and/or graphics, which may alter content. The journal's standard [Terms & Conditions](#) and the [Ethical guidelines](#) still apply. In no event shall the Royal Society of Chemistry be held responsible for any errors or omissions in this *Accepted Manuscript* or any consequences arising from the use of any information it contains.

Highly Efficient Polymer Solar Cells Based on a Universal Cathode Interlayer Composed of Metallophthalocyanine Derivative with Good Film-Forming Property

Cite this: DOI: 10.1039/x0xx00000x

Received 00th January 2012,
Accepted 00th January 2012

DOI: 10.1039/x0xx00000x

www.rsc.org/

Tao Jia, Weilong Zhou, Youchun Chen, Jianxiong Han, Lu Wang, Fenghong Li* and Yue Wang*

A new cathode interlayer (CIL) material metallophthalocyanine (MPc) derivative 1,4,8,11,15,18,22,25-octaalkoxy-2,3,9,10,16,17,23,24-octa-[N-methyl-(3-pyridyloxy)] zinc-phthalocyanine iodide (1:8) ($\text{ZnPc}(\text{OC}_8\text{H}_{17}\text{OPyCH}_3\text{I})_8$) was synthesized and applied in polymer solar cells (PSCs) based on PTB7:PC₇₁BM (PTB7 = thieno[3,4-b]thiophene/benzodithiophene, PC₇₁BM = [6,6]-phenyl C71-butyric acidmethyl ester), P3HT:PC₆₁BM (P3HT = poly(3-hexylthiophene), PC₆₁BM = [6,6]-phenyl C61-butyric acidmethyl ester) or PCDTBT:PC₇₁BM (PCDTBT = poly[N-9''-heptadecanyl-2,7-carbazole-alt-5,5-(4',7'-di-2-thienyl-2',1',3'-benzothiadiazole)]) as an active layer. As a result, power conversion efficiency (PCE) values of the PSCs are 8.52%, 4.02% and 6.88%, respectively, which are much higher than those of the corresponding PSCs with the Al-only cathode. It indicates that $\text{ZnPc}(\text{OC}_8\text{H}_{17}\text{OPyCH}_3\text{I})_8$ is a new promising candidate as a universal CIL for highly efficient PSCs. Compared to VOPc(OPyCH₃I)₈ (2,3,9,10,16,17,23,24-Octakis-[N-methyl-(3-pyridyloxy)] vanadylphthalocyanine iodide (1:8)), the PSC with $\text{ZnPc}(\text{OC}_8\text{H}_{17}\text{OPyCH}_3\text{I})_8$ as a CIL has higher short circuit current and fill factor because $\text{ZnPc}(\text{OC}_8\text{H}_{17}\text{OPyCH}_3\text{I})_8$ can form a better, denser and more uniform film on the active layer than VOPc(OPyCH₃I)₈ as demonstrated by atomic force microscopy (AFM), energy dispersive spectrum mapping on the scan electron microscopy (SEM-EDS mapping) and contact angle measurements.

1. Introduction

1. Introduction

Polymer solar cells (PSCs) have drawn great attention owing to their key advantages of synthetic variability, light weight, low cost, large-area roll to roll fabrication and the lucrative possibility of integration directly into flexible devices.¹ Power conversion efficiency (PCE) of the PSCs has rapidly increased to over efficiencies of 9% with good ambient stability for single cell devices.² One of efficient strategies to achieve such a high efficiency was the application of an alcohol/water soluble cathode interlayer (CIL) in the PSCs.^{2a-c} This kind of CIL was firstly used as an electron injection layer in polymer light-emitting diodes³ and then applied to organic field effect transistors⁴ and recently in the PSCs.^{2a-c, 5, 6} Currently reported CILs improving the device performance mainly consist of polymers⁵ and organic small molecules.⁶ Most of alcohol/water soluble polymer CILs have been designed and synthesized based on fluorine unit with alcohol/water soluble groups.^{2a-c, 5a-i} Some alcohol/water soluble polymers based on

trimethylammoniumhexylthiophene have also been used as CILs to construct highly efficient PSCs.^{5j, 5k} In addition, some organic small molecules were utilized as CILs in the PSCs as well.⁶ Successful alcohol/water soluble small molecular CILs include fullerene derivatives^{6a-d}, perylene diimides,^{6e, 6f} porphyrin,^{6g} pyridinium salt,^{6h} rhodamine with inner salt,⁶ⁱ quinacridone tethered with sodium sulfonate,^{6j} triphenylamine-uorene core featuring a phosphonate side chain,^{6k} tetra-n-alkyl ammonium bromides,^{6l} metallophthalocyanine (MPc) derivative⁷ and so on. Compared to polymers, the small molecules have advantages of well-defined structures, high-purity without batch-to-batch variation and easy modification. However it is more difficult for alcohol/water soluble small molecular CILs to form a high-quality uniform film than polymer CIL, in particular on the hydrophobic active layer.

For fabrication of PSCs with CIL by solution processing, to prevent intermixing between the active layer and the interlayer, the active layer must be sufficiently resistant against the solvent used for the CIL (conventional PSCs) or the CIL must be sufficiently resistant against the solvent used for the active layer (inverted PSCs). Because the active layers

were prepared by weak polar organic solvents and highly hydrophobic, the CIL materials must be soluble well in strongly polar solvents such as water or alcohol and are often greatly hydrophilic. The wettability of CIL materials on the surface of active layer is often very poor and with the terms reversed. On the above premise, it is very hard to prepare uniform thin CIL on the top surface of active layer. However, it is essential to construct a continuous, stable and well-distributed dipoles layer (CIL) between active layer and cathode for highly efficient PSCs. More importantly, the CIL should be endowed with characteristic that can promote electric and physical contact between active layer and metal cathode. The design and synthesis of CIL materials that can form uniformly electrical and physical adhesion between active layer and metal cathode still is a great challenge to further improve the PCE of PSCs.

Recently we reported a water-soluble MPc with pyridine salts VOPc(OPyCH₃I)₈ (Fig 1a) as a CIL leading to a simultaneous enhancement in open circuit voltage (V_{oc}), short circuit current (J_{sc}) and fill factor (FF) of the PSCs. As a result, a PCE of 8.12% for the working areas of 2 × 2 mm² and a PCE of 7.23% for the working areas of 4 × 4 mm² have been achieved. However, VOPc(OPyCH₃I)₈-treated surface of PTB7:PC₇₁BM blend showed a rough morphology with a root-mean-square (RMS) roughness of 9.34 nm. Notably, there are some visible islands distributed over the surface. The formation mechanism of the islands may be the self-aggregation of VOPc(OPyCH₃I)₈ itself due to its high polarity and adverse wettability of VOPc(OPyCH₃I)₈ aqueous solution on the hydrophobic active layer. Moreover, we found that RMS roughness of VOPc(OPyCH₃I)₈-treated surface of PTB7:PC₇₁BM increased with the development of time.⁷ Such a rough morphology is usually unfavorable for the device efficiency, especially for J_{sc}, FF and stability. Therefore, it is necessary to improve film formation of alcohol/water soluble

small molecular CILs on hydrophobic active layer in order to further increase device performance of the PSCs.

In this contribution, a new CIL material α -alkoxy substituted MPc derivative ZnPc(OC₈H₁₇OPyCH₃I)₈ has been intentionally synthesized by introducing eight alkoxy chains on the rigid skeleton as shown in Fig 1b. Such chemical modification provides the molecule with an ideal balance between the solubility in polar solvent and adhesive property on active layer surface. High conformational flexibility of the alkoxy chains affords the MPc derivative sufficient solubility in alcohol and hardly soluble in water, which makes it possess better wettability on the hydrophobic active layers. The abundant flexible alkoxy chains attached to the centre core of ZnPc(OC₈H₁₇OPyCH₃I)₈ promote uniform film formation on the lying organic layer. It was demonstrated that methanol/ethanol treatment can improve the performance of the PSCs due to passivation of surface traps and a corresponding increase of surface charge density of the active layer.⁸ Therefore a further enhanced PCE would be expected by spin-coating a ZnPc(OC₈H₁₇OPyCH₃I)₈ solution in methanol/ethanol on the active layer.

2. Results and discussion

Detailed UV/vis absorption spectrum and electrochemical properties of ZnPc(OC₈H₁₇OPyCH₃I)₈ are shown in the electronic supplementary information. We used ZnPc(OC₈H₁₇OPyCH₃I)₈ as a CIL in the PSCs based on a blend of PTB7 and PC₇₁BM as an active layer and Al as a cathode. Device architecture is presented in Fig 1c.

ZnPc(OC₈H₁₇OPyCH₃I)₈ can be dissolved well in alcohol (methanol or ethanol) while its solubility in other common organic solvents such as chloroform, chlorobenzene, tetrahydrofuran and toluene is very poor. The optimized concentration of ZnPc(OC₈H₁₇OPyCH₃I)₈ in methanol was 0.8

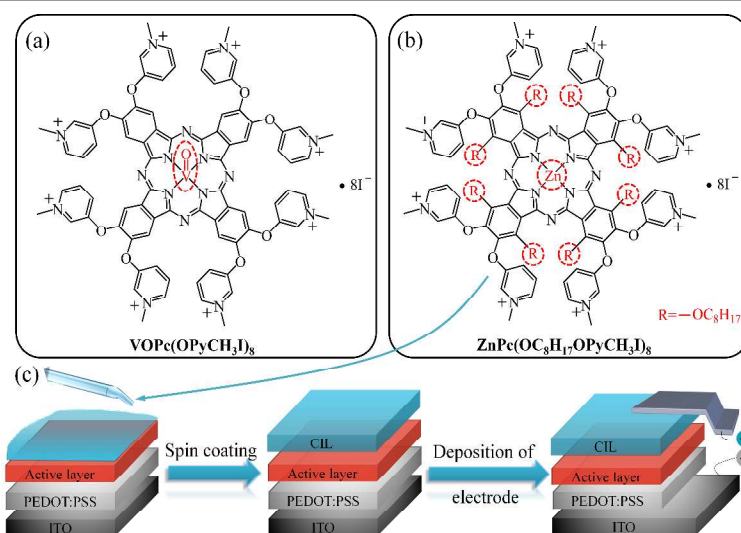


Figure 1. Molecular structures of (a) VOPc(OPyCH₃I)₈, (b) ZnPc(OC₈H₁₇OPyCH₃I)₈ and (c) device configuration of PSCs with a CIL. Difference between VOPc(OPyCH₃I)₈ (a) and ZnPc(OC₈H₁₇OPyCH₃I)₈ (b) is highlighted in red font and marked by red dash circles.

mg mL⁻¹. For comparison, two control devices without (Device 1) and with (Device 2) methanol treatment at the interlayer between the PTB7:PC₇₁BM and Al have been fabricated. Fig. 2 presents current density–voltage (*J–V*) characteristics of the two control devices and the PSCs with ~ 5nm ZnPc(OC₈H₁₇OPyCH₃I)₈ as a CIL (Device 3) under AM 1.5G illumination at 100 mW cm⁻². *J–V* curves of the three devices in the dark are presented in Fig. 3. Table 1 summarizes the device performance parameters derived from Fig. 2. Intriguingly, PCE of Device 3 with the ZnPc(OC₈H₁₇OPyCH₃I)₈ as a CIL can reach 8.52% which is higher than not only ones of the two control devices but also PCE (8.12%) of Device R with ~ 5nm VOPc(OPyCH₃I)₈ as a CIL.⁷ Compared to the two control devices, introduction of ZnPc(OC₈H₁₇OPyCH₃I)₈ between active layer and cathode results in a simultaneous enhancement in Voc, Jsc and FF. Moreover the Device 3 has even higher Jsc and FF than Device R. The results should be attributed to an excellent film-forming property of ZnPc(OC₈H₁₇OPyCH₃I)₈ on the active layer by spin-coating the solution of ZnPc(OC₈H₁₇OPyCH₃I)₈ in methanol. In order to ensure the validity and repeatability of data, we measured at least 30 pixels (size = 2 × 2 mm²) for all device configurations. The average PCE values of Device 1 – 3 are 5.06%, 6.51% and 8.46%, respectively. In order to detect a discrepancy of Jsc which easily leads to overvalued PCE,⁹ external quantum efficiency (EQE) spectra of the Devices 1 – 3 from 350 nm to 800 nm were carried out and shown in Fig. 4. Jsc values calculated from integration of the EQE spectra are 13.93 mA cm⁻² for Device 1, 15.11 mA cm⁻² for Device 2 and 16.47 mA cm⁻² for Device 3, which are in good agreement with Jsc = 13.98 mA cm⁻² of Device 1 (ca. 0.3% error), Jsc = 15.34 mA cm⁻² of Device 2 (ca. 1.5% error) and Jsc = 16.88 mA cm⁻² of Device 3 (ca. 2.4% error) obtained from *J–V* characteristics under illumination. It indicates that the Jsc values measured for the PSCs are reliable and PCE values presented in this manuscript are not overvalued.

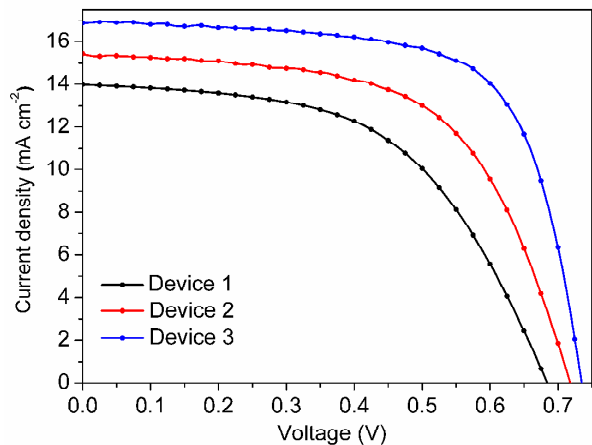


Figure 2. Current density versus voltage (*J–V*) characteristics of devices with ZnPc(OC₈H₁₇OPyCH₃I)₈ (blue line, Device 3) as a CIL, with (red line, Device 2) and without (black line, Device 1) methanol treatment at the surface of PTB7:PC₇₁BM under 100 mW cm⁻² AM 1.5G illumination.

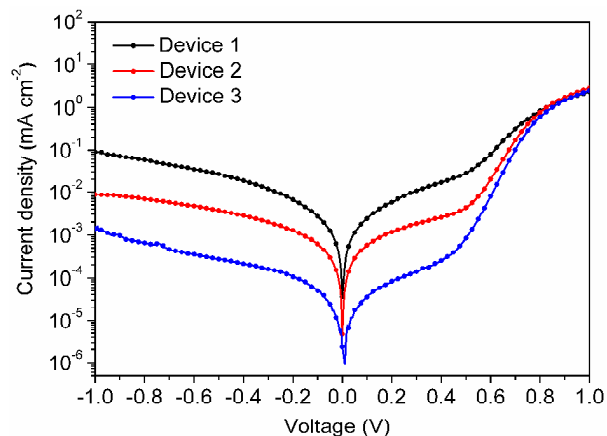


Figure 3. *J–V* characteristics of the Device 1 (black line), Device 2 (red line) and Device 3 (blue line) in the dark.

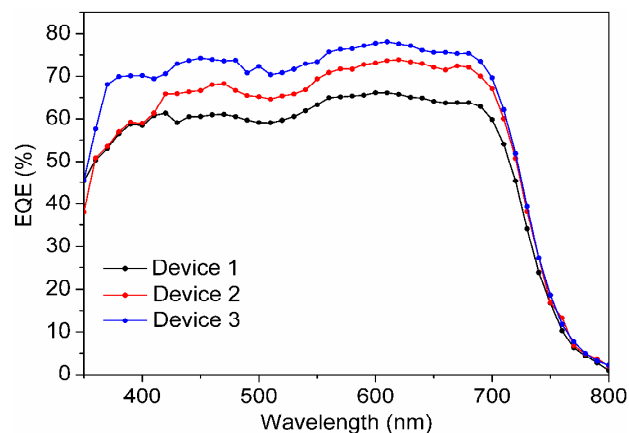


Figure 4. EQE spectra of the Device 1 (black line), Device 2 (red line) and Device 3 (blue line).

Under illumination, Device 3 with ZnPc(OC₈H₁₇OPyCH₃I)₈ as a CIL showed a Voc of 0.738 V which is higher than the control devices with (Voc = 0.715 V, Device 2) and without (Voc = 0.679 V, Device 1) methanol treatment. The increase in Voc can be mainly attributed to the reduced work function (WF) of Al cathode. Ultraviolet photoemission spectroscopic (UPS) measurements were carried out with monochromatized HeI radiation at 21.2 eV. WF is defined by secondary electron cutoff in the UPS spectra of Al, Al treated by methanol and Al covered by ZnPc(OC₈H₁₇OPyCH₃I)₈ as shown in Fig. S3. As a result, the WF values are 4.12 eV for bare Al, 3.55 eV for Al treated by methanol and 3.32 eV for Al covered by ZnPc(OC₈H₁₇OPyCH₃I)₈. Unsurprisingly, the Voc of Device 3 is almost the same with the Voc of the Device R due to a close WF value (3.30 eV) for Al covered by VOPc(OPyCH₃I)₈. The increased Voc is consistent with the increased built-in potential across devices with CIL. This speculation can be supported by the dark *J–V* characteristics of devices in Fig. 3. In the dark, Devices 3 exhibit a turn-on voltage around 0.78 V while they are around 0.76 V for Device 2 and 0.71 V for the Device 1, respectively. It suggests that the built-in voltage (*V_{bi}*) (here considered as flat-band condition) of the devices increase when

introducing $\text{ZnPc}(\text{OC}_8\text{H}_{17}\text{OPyCH}_3\text{I})_8$ as a CIL or methanol treatment. Because V_{bi} influences the internal electric field in polymer bulk heterojunction (BHJ) solar cells and gives the upper limit for the V_{oc} provided that the WF difference of electrodes is larger than the donor HOMO-acceptor LUMO offset of the BHJ. Thus the increase of V_{bi} may be responsible for the increase in V_{oc} in the Device 3 and Device 2.

In order to confirm that introducing $\text{ZnPc}(\text{OC}_8\text{H}_{17}\text{OPyCH}_3\text{I})_8$ film not only enhances electron transport but also facilitates a balance of electron and hole transport in the PSCs, the mobilities of electron and hole were measured in the electron-only and hole-only devices using space charge limited current (SCLC) method (details and parameters in Fig. S4a, S4b and Table S2). The mobilities of electron and hole for the devices without any treatment at the interlayer between the PTB7:PC₇₁BM and Al are $1.35 \times 10^{-5} \text{ cm}^2 \text{ V}^{-1} \text{ s}$ and $3.25 \times 10^{-4} \text{ cm}^2 \text{ V}^{-1} \text{ s}$, respectively. However, the mobilities of electron and hole for the devices with $\text{ZnPc}(\text{OC}_8\text{H}_{17}\text{OPyCH}_3\text{I})_8$ as a CIL are $3.29 \times 10^{-4} \text{ cm}^2 \text{ V}^{-1} \text{ s}$ and $4.12 \times 10^{-4} \text{ cm}^2 \text{ V}^{-1} \text{ s}$, respectively. It is apparent that incorporation of the CIL increases the electron mobility up to one order of magnitude and a perfect mobility balance of hole and electron has been achieved.

Table 1. The performances of PTB7:PC₇₁BM PSCs with the various cathodes.

Device	V_{oc} [v]	J_{sc} [mA cm ⁻²]	FF [%]	PCE [%]		R_{s} [Ω cm ²]	R_{sh} [Ω cm ²]
				Max	Aver		
R	0.740	16.60	66.0	8.12	8.05	6.2	1300
1	0.679	13.98	54.0	5.12	5.06	13.7	751
2	0.715	15.34	60.1	6.59	6.51	8.4	1001
3	0.738	16.88	68.4	8.52	8.46	4.6	1587
4	0.720	15.59	61.0	6.85	6.76	8.1	1050
5	0.745	16.45	66.0	8.10	8.06	5.1	1580

Device R: [ITO/PEDOT:PSS/PTB7:PC₇₁BM/VOPc(OPyCH₃I)₈/Al]

Device 1: [ITO/PEDOT:PSS/PTB7:PC₇₁BM/Al]

Device 2: [ITO/PEDOT:PSS/PTB7:PC₇₁BM/methanol/Al]

Device 3: [ITO/PEDOT:PSS/PTB7:PC₇₁BM/ZnPc(OC₈H₁₇OPyCH₃I)₈ (in methanol)/Al]

Device 4: [ITO/PEDOT:PSS/PTB7:PC₇₁BM/ethanol/Al]

Device 5: [ITO/PEDOT:PSS/PTB7:PC₇₁BM/ZnPc(OC₈H₁₇OPyCH₃I)₈ (in ethanol)/Al]

Table 1 also presents series resistances (R_{s}) and shunt resistances (R_{sh}) of the devices obtained from the slopes of J - V curves at V_{oc} and J_{sc} , respectively. Compared to the two control devices and Device R, a decrease of R_{s} and an increase of R_{sh} are apparent when $\text{ZnPc}(\text{OC}_8\text{H}_{17}\text{OPyCH}_3\text{I})_8$ was utilized as a CIL. More importantly compared to the Device R with VOPc(OPyCH₃I)₈ as a CIL, the increases of J_{sc} and FF of the Device 3 are attributed to the resistance changes due to formation of a high-quality uniform film of $\text{ZnPc}(\text{OC}_8\text{H}_{17}\text{OPyCH}_3\text{I})_8$ on PTB7:PC₇₁BM.

Fig. 5 shows the surface morphologies obtained by atomic force microscopy (AFM) measured at ambient. The surface of PTB7:PC₇₁BM film is smooth with a root-mean-square (RMS) roughness of 2.79 nm (Fig. 5a). The methanol-treated surface of PTB7:PC₇₁BM was slightly smoother than the pristine film due to a

RMS roughness of 2.04 nm and remained homogeneous as shown Fig. 5b. When a PTB7:PC₇₁BM blend is covered by $\text{ZnPc}(\text{OC}_8\text{H}_{17}\text{OPyCH}_3\text{I})_8$ film, the RMS roughness of the surface becomes 1.91 nm (Fig. 5c) which is much smoother than VOPc(OPyCH₃I)₈ on PTB7:PC₇₁BM with RMS roughness of 9.34 nm (Fig. 5d) and even smoother than pristine and methanol-treated surfaces of PTB7:PC₇₁BM. Moreover $\text{ZnPc}(\text{OC}_8\text{H}_{17}\text{OPyCH}_3\text{I})_8$ has a better film-forming property on PTB7:PC₇₁BM blend than famous alcohol soluble polymer PFN, because the RMS roughness of PFN on the PTB7:PC₇₁BM is 3.41 nm (Fig. S5). Notably, $\text{ZnPc}(\text{OC}_8\text{H}_{17}\text{OPyCH}_3\text{I})_8$ film has solved the problem with sharp island formation of MPc derivatives, e.g. VOPc(OPyCH₃I)₈ on the hydrophobic active layer. We assign it to the introduction of eight alkoxy chains which can enhance the compatibility and adhesive characteristic between active layer and $\text{ZnPc}(\text{OC}_8\text{H}_{17}\text{OPyCH}_3\text{I})_8$ based CIL.

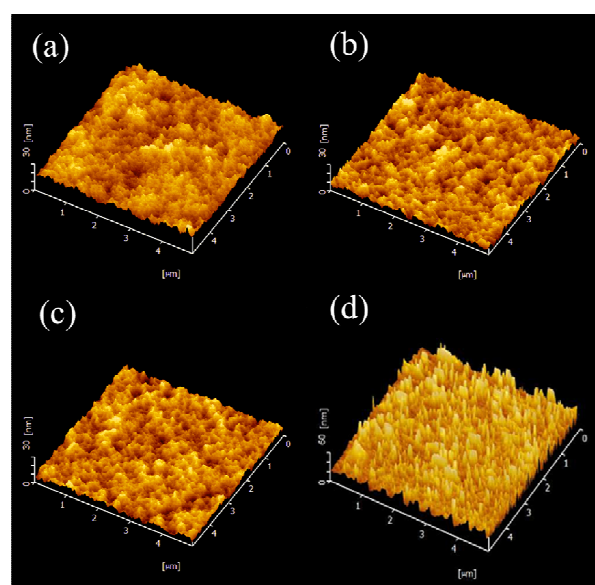


Figure 5. AFM images of (a) PTB7:PC₇₁BM film; (b) PTB7:PC₇₁BM film with methanol treatment; (c) $\text{ZnPc}(\text{OC}_8\text{H}_{17}\text{OPyCH}_3\text{I})_8$ on PTB7:PC₇₁BM film; (d) VOPc(OPyCH₃I)₈ on PTB7:PC₇₁BM film.

In order to further prove that $\text{ZnPc}(\text{OC}_8\text{H}_{17}\text{OPyCH}_3\text{I})_8$ has better film formation and more uniform distribution on the active layer than VOPc(OPyCH₃I)₈, we detected distributions of metal elements and iodine element of the two molecules on the active layer using energy dispersive spectrum mapping on the scan electron microscopy (SEM-EDS mapping). SEM-EDS mapping images of $\text{ZnPc}(\text{OC}_8\text{H}_{17}\text{OPyCH}_3\text{I})_8$ on PTB7:PC₇₁BM film are shown in Fig. 6(a) where the purple dots are zinc (Zn) element and Fig. 6(b) where the blue dots are iodine (I) element. Fig. 6c is a combination of the maps of Zn element in Fig. 6a and I element in Fig. 6b. In the same way, SEM-EDS mapping images of VOPc(OPyCH₃I)₈ on PTB7:PC₇₁BM film are shown in Fig. 6(d) where the yellow dots are vanadium (V) element and Fig. 6(e) where the blue dots are I element. Fig. 6f is a combination of the maps of V element in Fig. 6d and I element in Fig. 6e. Apparently massive dots for elements of $\text{ZnPc}(\text{OC}_8\text{H}_{17}\text{OPyCH}_3\text{I})_8$ have densely covered background for PTB7:PC₇₁BM in Fig. 6c. However, dots for

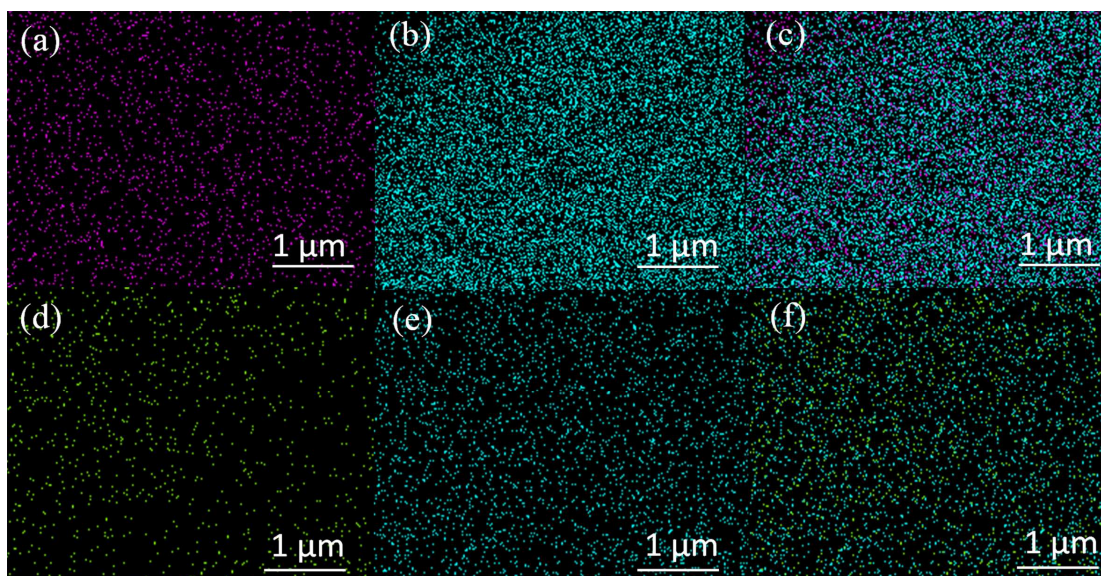


Figure 6. SEM-EDS mapping images of $\text{ZnPc}(\text{OC}_8\text{H}_{17}\text{OPyCH}_3\text{I})_8$ on PTB7:PC₇₁BM film are shown in (a) where purple dots are zinc element, (b) where blue dots are iodine element and (c) which is a combination of (a) and (b); SEM-EDS mapping images of $\text{VOPc}(\text{OPyCH}_3\text{I})_8$ on PTB7:PC₇₁BM film are shown in (d) where yellow dots are vanadium element, (e) where blue dots are iodine element and (f) which is a combination of (d) and (e).

elements of $\text{VOPc}(\text{OPyCH}_3\text{I})_8$ are much sparser and a large area of the background is uncovered as shown in Fig. 6f. It is strongly evident that $\text{ZnPc}(\text{OC}_8\text{H}_{17}\text{OPyCH}_3\text{I})_8$ can form a better, denser and more uniform film on the active layer than $\text{VOPc}(\text{OPyCH}_3\text{I})_8$.

In addition, contact angle (θ) measurements were performed in order to investigate polarity of treated surfaces of PTB7:PC₇₁BM film and the wetting property of $\text{ZnPc}(\text{OC}_8\text{H}_{17}\text{OPyCH}_3\text{I})_8$ in methanol and $\text{VOPc}(\text{OPyCH}_3\text{I})_8$ in water on PTB7:PC₇₁BM film as shown in Fig. 7. Fig. 7a – 7d show contact angle images of water droplets on the surfaces of PTB7:PC₇₁BM film without and with methanol treatment, covered by $\text{ZnPc}(\text{OC}_8\text{H}_{17}\text{OPyCH}_3\text{I})_8$ and $\text{VOPc}(\text{OPyCH}_3\text{I})_8$, respectively. The water contact angles of the four surfaces are 99.5°, 97.6°, 92.8°, 55.6°, respectively. It indicates that the treatments of both methanol and $\text{ZnPc}(\text{OC}_8\text{H}_{17}\text{OPyCH}_3\text{I})_8$ only slightly changed the surface polarity of PTB7:PC₇₁BM. The surfaces of PTB7:PC₇₁BM/ $\text{ZnPc}(\text{OC}_8\text{H}_{17}\text{OPyCH}_3\text{I})_8$ is still hydrophobic due to $\theta \approx 92.8^\circ$. However, the surface of PTB7:PC₇₁BM/ $\text{VOPc}(\text{OPyCH}_3\text{I})_8$ is hydrophilic due to $\theta \approx 55.6^\circ$. Fig. 7e – 7g present photos of liquid droplets of methanol, $\text{ZnPc}(\text{OC}_8\text{H}_{17}\text{OPyCH}_3\text{I})_8$ in methanol and $\text{VOPc}(\text{OPyCH}_3\text{I})_8$ in water on the surfaces of PTB7:PC₇₁BM. The contact angles of the three liquid droplets are 7.7°, 10.5°, 88.3°, which strongly suggest that wetting property of $\text{ZnPc}(\text{OC}_8\text{H}_{17}\text{OPyCH}_3\text{I})_8$ in methanol is much better than $\text{VOPc}(\text{OPyCH}_3\text{I})_8$ in water on PTB7:PC₇₁BM film. The contact angle measurements once more provide a powerful proof that $\text{ZnPc}(\text{OC}_8\text{H}_{17}\text{OPyCH}_3\text{I})_8$ has a larger potential to form a high-quality film on the active layer than $\text{VOPc}(\text{OPyCH}_3\text{I})_8$.

The surface energy of various films can be calculated based on contact angle measurements according to the equations from the “Three-Liquid Acid-Base Methode”.¹⁰ Ma et al. has obtained the surface energies of ITO, P3HT, PC₆₁BM, P3HT:PC₆₁BM, PCBDAN and P3HT:PC₆₁BM:PCBDAN using the method.¹¹ To further investigate the effect of the two MPc

derivatives on the surface energy of the active layer, we also carried out advancing contact angle measurements by selecting water, ethylene glycol and hexadecane as probing liquids. Table 2 presents our results for measured contact angles and calculated surface energies and their components. The surface energy of ITO is 38.0 mN m⁻¹, which is similar to the value (40.0 mN m⁻¹) reported by Ma et al.¹¹ The surface energies of PTB7:PC₇₁BM (25.2 mN m⁻¹) and PTB7:PC₇₁BM/ $\text{ZnPc}(\text{OC}_8\text{H}_{17}\text{OPyCH}_3\text{I})_8$ (26.1 mN m⁻¹) are quite close each other. However the surface energy of PTB7:PC₇₁BM/ $\text{VOPc}(\text{OPyCH}_3\text{I})_8$ changes to 38.7 mN m⁻¹, which is even higher than one of ITO though $\text{VOPc}(\text{OPyCH}_3\text{I})_8$ only partially covered PTB7:PC₇₁BM as shown in Fig. 6f. It proves $\text{ZnPc}(\text{OC}_8\text{H}_{17}\text{OPyCH}_3\text{I})_8$ has a better wettability and compatibility on the active layer than $\text{VOPc}(\text{OPyCH}_3\text{I})_8$.

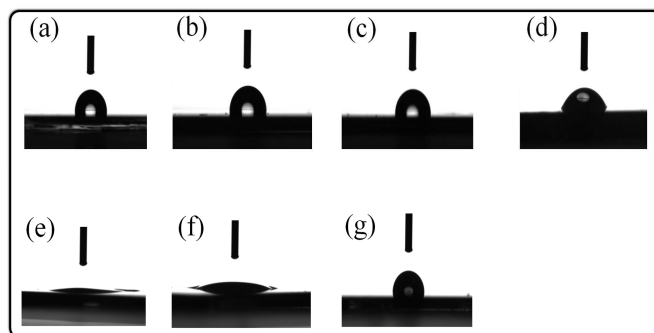


Figure 7. Contact angle measurements. Photos of water droplets on the surfaces of (a) PTB7:PC₇₁BM film; (b) PTB7:PC₇₁BM film treated by methanol; (c) $\text{ZnPc}(\text{OC}_8\text{H}_{17}\text{OPyCH}_3\text{I})_8$ on PTB7:PC₇₁BM film and (d) $\text{VOPc}(\text{OPyCH}_3\text{I})_8$ on PTB7:PC₇₁BM film. Photos of liquid droplets of (e) methanol; (f) $\text{ZnPc}(\text{OC}_8\text{H}_{17}\text{OPyCH}_3\text{I})_8$ in methanol and (g) $\text{VOPc}(\text{OPyCH}_3\text{I})_8$ in water on the surfaces of PTB7:PC₇₁BM.

Table 2. Advancing contact angles of three probing liquids on various surfaces at initial state and the calculated surface energies (mN m^{-1})

		ITO	PTB7:PC ₇₁	PTB7:PC ₇₁ BM/ BM	PTB7:PC ₇₁ BM/ VOPc(OPyCH ₃) ₈
Contact angle (deg)	Water	14.2±1	99.5±1	92.8±1	55.6±1
	Ethylene Glycol	31.5±1	70.7±1	65.2±1	35.7±1
	Hexadecane	13.0±1	32.3±1	31.9±1	41.5±1
Calculated surface energy component (mN m^{-1})	γ	38.0	25.2	26.1	38.7
	γ^{LW}	26.8	23.4	23.5	21.0
	γ^{AB}	11.2	1.82	2.57	17.7
	γ^+	0.41	0.15	0.72	2.68
	γ^-	76.9	5.52	2.30	29.3

γ is the surface energy, γ^{LW} refers to the Lifshitz-van der Waals interaction and γ^{AB} refers to the acid-base interaction. γ^+ and γ^- stand for the Lewis acid and base parameters of surface energy.

Encouraged by successful application of $\text{ZnPc}(\text{OC}_8\text{H}_{17}\text{OPyCH}_3)_8$ as a CIL in PSCs with the PTB7:PC₇₁BM as an active layer, the MPc derivative was also introduced into the PSCs based on P3HT:PC₆₁BM and PCDTBT:PC₇₁BM to demonstrate its universality acting as a CIL in PSCs. Table 3 lists a summary of the device performance parameters derived from $J-V$ curves of devices with P3HT:PC₆₁BM and PCDTBT:PC₇₁BM as the active layer under 100 mW cm^{-2} AM 1.5G illumination (see Fig. S6 and S7). In the case of P3HT:PC₆₁BM blends, incorporating $\text{ZnPc}(\text{OC}_8\text{H}_{17}\text{OPyCH}_3)_8$ as a CIL led to a great increase of PCE from 2.17% (Device I) to 4.02% (Device II) due to increases of Voc from 0.488 V to 0.604 V, Jsc from 9.22 mA cm^{-2} to 10.05 mA cm^{-2} , FF from 48.2% to 66.2%. Similarly $\text{ZnPc}(\text{OC}_8\text{H}_{17}\text{OPyCH}_3)_8$ as a CIL in the PSCs based on PCDTBT:PC₇₁BM gave rise to a simultaneous increase of Voc, Jsc and FF compared to the control device without a CIL. As a result, PCE enhanced from 5.34% (Device III) to 6.88% (Device IV).

Table 3. Performances of the PSCs based on P3HT:PC₆₁BM, PCDTBT:PC₇₁BM with the various cathodes.

Device	Voc [V]	Jsc [mA cm^{-2}]	FF [%]	PCE [%]		Rs [Ωcm^2]	Rsh [Ωcm^2]
				Max	Aver		
I	0.488	9.22	48.2	2.17	2.08	13.2	312
II	0.604	10.05	66.2	4.02	3.98	8.4	5882
III	0.868	10.95	56.2	5.34	5.26	15.7	505
IV	0.920	11.63	64.3	6.88	6.78	7.1	920

Device I: [ITO/PEDOT:PSS/P3HT:PC₆₁BM/Al]

Device II: [ITO/PEDOT:PSS/P3HT:PC₆₁BM/ $\text{ZnPc}(\text{OC}_8\text{H}_{17}\text{OPyCH}_3)_8$ /Al]

Device III: [ITO/PEDOT:PSS/PCDTBT:PC₇₁BM/Al]

Device IV: [ITO/PEDOT:PSS/PCDTBT:PC₇₁BM/ $\text{ZnPc}(\text{OC}_8\text{H}_{17}\text{OPyCH}_3)_8$ /Al]

Finally, ethanol also was employed as solvent of $\text{ZnPc}(\text{OC}_8\text{H}_{17}\text{OPyCH}_3)_8$ to fabricate PSCs with PTB7:PC₇₁BM as the active layer (see Fig. S8). For Device 4 ethanol treatment was performed at the interlayer between the PTB7:PC₇₁BM and Al and for Device 5 the CIL was prepared from the ethanol solution of $\text{ZnPc}(\text{OC}_8\text{H}_{17}\text{OPyCH}_3)_8$. The PCEs of Devices 4 and 5 are 6.85% and 8.10%, respectively. The detail parameters of Devices 4 – 5 are listed in Table 1. The $\text{ZnPc}(\text{OC}_8\text{H}_{17}\text{OPyCH}_3)_8$ film as a CIL prepared from ethanol solution can also remarkably enhance the performance of the PSCs. These results suggest a possible approach to fabricate high-performance PSCs with greener solvents.

3. Conclusions

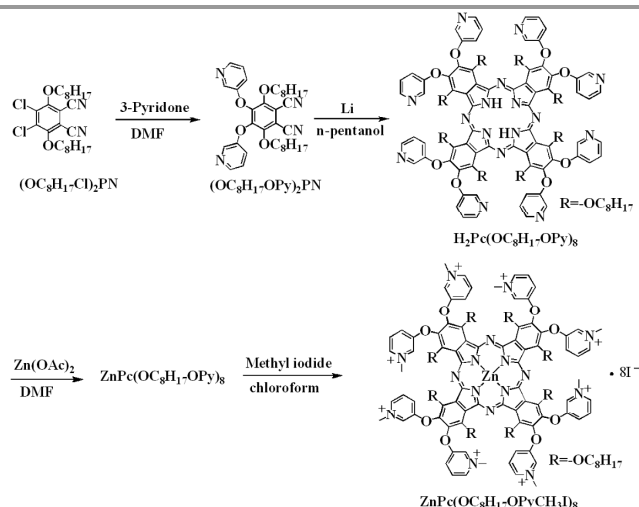
In conclusion, a new metallophthalocyanine (MPc) derivative, $\text{ZnPc}(\text{OC}_8\text{H}_{17}\text{OPyCH}_3)_8$, has been synthesized and successfully utilized as a CIL in the PSCs based on PTB7:PC₇₁BM, P3HT:PC₆₁BM and PCDTBT:PC₇₁BM. A simultaneous increase of Voc, Jsc and FF resulted in an overall PCE enhancement due to an introduction of $\text{ZnPc}(\text{OC}_8\text{H}_{17}\text{OPyCH}_3)_8$. As a result, max. PCE values of the PSCs based on PTB7:PC₇₁BM, P3HT:PC₆₁BM, and PCDTBT:PC₇₁BM were 8.52%, 4.02% and 6.88%, respectively. It indicates that $\text{ZnPc}(\text{OC}_8\text{H}_{17}\text{OPyCH}_3)_8$ is a new promising candidate as a good CIL for highly efficient PSCs. Compared to VOPc(OPyCH₃)₈, $\text{ZnPc}(\text{OC}_8\text{H}_{17}\text{OPyCH}_3)_8$ realized the uniform deposition on the lying organic layer due to introducing the flexible alkoxy chains. Such a chemical modification can enhance the compatibility and adhesive characteristic between active layer and $\text{ZnPc}(\text{OC}_8\text{H}_{17}\text{OPyCH}_3)_8$ -based CIL and meanwhile improve solubility in alcohol. So the interlayer material displayed better wettability on the hydrophobic active layer. For phthalocyanine

molecules, the structural modification space is very wide. Therefore it should be an efficient strategy to improve the film formation for highly efficient PSCs.

4. Experimental section

4.1 Synthesis and characterization

Materials and Methods: ^1H NMR spectra were measured on a Varian Mercury 300 MHz spectrometer (USA) with tetramethylsilane as the internal standard. Elemental analyses were performed on a flash EA 1112 spectrometer (Germany). MALDI-TOF mass spectra were recorded on Kratos AXIMA-CFR Kompact MALDI Mass Spectrometer with anthracene-1,8,9-triol as the matrix. All reagents and solvents, unless otherwise specified, were obtained from Aldrich (USA) and Acros (Belgium) and used as received. P3HT was purchased from Rieke Metals Inc (USA), PCDTBT and PTB7 were purchased from 1-Material Inc (Canada). PC₆₁BM and PC₇₁BM were purchased from American Dye Source (USA). All reactions were carried out using Schlenk techniques under a nitrogen atmosphere. 4,5-Dichloro-3,6-bis(octyloxy)phthalonitrile ((OC₈H₁₇Cl)₂PN) was prepared according to the literature methods.¹²



Scheme 1 Synthesis of ZnPc(OC₈H₁₇OPyCH₃)₈.

3,6-Bis(octyloxy)-4,5-bis(3-pyridyloxy) phthalonitrile ((OC₈H₁₇OPy)₂PN): (OC₈H₁₇Cl)₂PN (4.52 g, 10.0 mmol), 3-pyridone (2.38 g, 25.0 mmol) and potassium carbonate (8.28 g, 60.0 mmol) were dissolved in 100 ml dry DMF under nitrogen atmosphere and the mixture was heated at 100 °C for 5 h. After cooling to room temperature, solvent was removed by vacuum evaporation and the crude product was purified by column chromatography using silica gel with dichloromethane and ethyl acetate as the eluents to obtain the yellowish liquid. Yield: 3.71 g (65%). ^1H NMR (300 MHz, CDCl₃, δ): 8.36 – 8.34 (m, 2 H), 8.15 – 8.14 (m, 2 H), 7.23 – 7.19 (m, 2 H), 7.03 – 6.99 (m, 2 H), 4.17 – 4.13 (t, J = 6.6 Hz, 4 H), 1.68 – 1.59 (m, 4 H), 1.29 – 1.21 (m, 20 H), 0.88 – 0.84 (t, J = 6.9 Hz, 6 H). MS (MALDI-TOF): m/z : 572.3

[M+H]⁺. Elemental analysis calcd: C 71.55%, H 7.42%, N 9.82%; found: C 71.53%, H 7.45%, N 9.86%.

1,4,8,11,15,18,22,25-Octaoctyloxy-2,3,9,10,16,17,23,24-octa-(3-pyridyloxy) phthalocyanine (H₂Pc(OC₈H₁₇OPy)₈): (OC₈H₁₇OPy)₂PN (2.85 g, 5.0 mmol) was dissolved in 20 ml dry n-pentanol and the mixture was heated at 100 °C for 5 min. Under nitrogen atmosphere, lithium (0.11 g, 15.0 mmol) was added, and then the mixture was refluxed for 2 h. After cooling to room temperature, solvent was removed by vacuum evaporation and the crude product was purified by column chromatography using silica gel with dichloromethane and ethyl acetate as the eluents to obtain the green powder. Yield: 293 mg (10%). ^1H NMR (300 MHz, CDCl₃, δ): 8.47 – 8.45 (m, 8 H), 8.34 – 8.32 (m, 8 H), 7.43 – 7.40 (m, 8 H), 7.28 – 7.24 (m, 8 H), 4.89 – 4.84 (t, J = 6.6 Hz, 16 H), 1.84 – 1.75 (m, 16 H), 1.28 – 1.11 (m, 80 H), 0.83 – 0.78 (t, J = 6.9 Hz, 24 H). MS (MALDI-TOF): m/z : 2285.2 [M+H]⁺. Elemental analysis calcd: C 71.49%, H 7.50%, N 9.81%; found: C 71.45%, H 7.48%, N 9.86%.

ZnPc(OC₈H₁₇OPyCH₃)₈: A solution of H₂Pc(OC₈H₁₇OPy)₈ (200 mg, 0.09 mmol) and zinc acetate (32 mg, 0.18 mmol) in 30 ml dry DMF was heated to reflux for 5 h. After cooling to room temperature, solvent was removed by vacuum evaporation, the crude product was purified by alumina oxide chromatography with dichloromethane and ethyl acetate as the eluents to obtain the green powder. Then the product (160 mg, 0.07 mmol) was dissolved in 20 ml dry chloroform. Under nitrogen atmosphere, methyl iodide (239 mg, 1.68 mmol) was added, the solution was stirred and heated to reflux for 2 h. After cooling to room temperature, the solvent was removed by vacuum evaporation, the crude product was purified by recrystallization with methanol and chloroform to obtain green powder. Yield: 226 mg (72%). ^1H NMR (300 MHz, DMSO-*d*₆, δ): 9.37 – 9.36 (m, 8 H), 8.96 – 8.94 (m, 8 H), 8.68 – 8.65 (m, 8 H), 8.25 – 8.20 (m, 8 H), 4.95 – 4.91 (t, J = 6.3 Hz, 16 H), 4.38 (s, 24H), 1.74 – 1.69 (m, 16 H), 1.24 – 1.08 (m, 80 H), 0.87 – 0.82 (t, J = 7.2 Hz, 24 H). MS (MALDI-TOF): m/z : 743.9 [M]⁴⁺. Elemental analysis calcd: C 49.65%, H 5.55%, N 6.43%; found: C 49.61%, H 5.58%, N 6.40%.

4.2 Device fabrication and characterization

ITO glass substrates were pre-cleaned carefully and treated with oxygen plasma for 7 min. Firstly PEDOT:PSS (Baytron PVP Al 4083) was spin-coated onto a cleaned ITO and annealed in air at 120 °C for 10 min. Secondly, blend films of active layers were spin-casted from solution on PEDOT:PSS. For P3HT:PC₆₁BM PSCs, the active layer was formed by spin-coating from *o*-dichlorobenzene (ODCB) solution consisting of 17 mg mL⁻¹ P3HT and 17 mg mL⁻¹ PC₆₁BM at 500 rpm for 18 s, followed by solvent annealing at room temperature for 2 h, and thermally annealing at 120 °C for 10 min. For PCDTBT:PC₇₁BM PSCs, the active layer was formed by spin-coating from the chlorobenzene:*o*-dichlorobenzene (1:3) solution consisting of 7 mg mL⁻¹ PCDTBT and 28 mg mL⁻¹ PC₇₁BM at 2000 rpm for 40 s, followed by thermally annealing at 75 °C for 10 min. For PTB7:PC₇₁BM PSCs, the active layer was formed by spin-coating from the chlorobenzene:1,8-diiodooctane (97:3 vol%) solution consisting of 10 mg mL⁻¹

PTB7 and 15 mg mL⁻¹ PC₇₁BM, then dried in vacuum. ZnPc(OC₈H₁₇OPyCH₃I)₈ was deposited on the active layer by spin-coating and then 100 nm Al was evaporated as a cathode. For the electron-only and hole-only devices, their device structures were: ITO/Al/PTB7:PC₇₁BM/with or without CIL/Al and ITO/PEDOT:PSS/PTB7:PC₇₁BM/with or without CIL/MoOx/Al, respectively. Current density-voltage (*J*-*V*) characteristics of the devices were measured under N₂ atmosphere in the glove box by using a Keithley 2400 under illumination and in the dark. Solar cell performance was tested under 1 sun, AM 1.5G full spectrum solar simulator (Photo Emission Tech. Inc., model #SS50AAA-GB) with an irradiation intensity of 100 mW cm⁻² calibrated with a standard silicon photovoltaic traced to the National institute of metrology, China. External quantum efficiency (EQE) spectra were measured using Q Test Station 2000 (Crowntech Inc. USA) at room temperature in air. In addition, the static contact angles of the as-prepared surfaces were measured with a commercial contact angle system (DataPhysics, OCA 20) at ambient temperature. AFM images were measured with an S II Nanonavi probe station 300 HV (Seiko, Japan) in contact mode. Scanning electron microscope (SEM) image was taken with a JEOL FESEM 6700F electron microscope with primary electron energy of 3 kV. Energy dispersive spectrum (EDS) mapping was conducted with Inca X-Max instruments made by Oxford Instruments.

Acknowledgements

This work was supported by grants from the National Basic Research Program of China (2014CB643500) and the Natural Science Foundation of China (51273077 and 51173065).

Notes and references

State Key Laboratory of Supramolecular Structure and Materials, Jilin University, Qianjin Avenue, Changchun, 130012, P. R. China.

Fax: XX XXXX XXXX; Tel: XX XXXX XXXX;

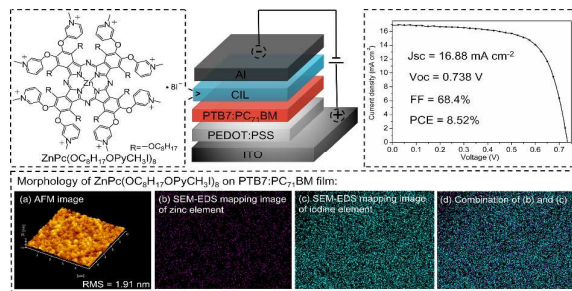
E-mail: fhli@jlu.edu.cn (F. H. Li); yuewang@jlu.edu.cn (Y. Wang)

† Electronic Supplementary Information (ESI) available: [details of UV/vis absorption spectrum and electrochemical properties of ZnPc(OC₈H₁₇OPyCH₃I)₈, *J*-*V* characteristics of electron-only and hole-only devices and curves of the PSCs based on P3HT:PC₆₁BM, PCDTBT:PC₇₁BM with the various cathodes.] See DOI: 10.1039/b000000x/

‡ Tao Jia and Weilong Zhou contributed equally to this work.

- (a) J. Peet, J. Y. Kim, N. E. Coates, W. L. Ma, D. Moses, A. J. Heeger & G. C. Bazan, *Nat. Mater.*, 2007, **6**, 497; (b) J. Y. Kim, K. Lee, N. E. Coates, D. Moses, T.-Q. Nguyen, M. Dante, A. J. Heeger, *Science*, 2007, **317**, 222; (c) S. H. Park, A. Roy, S. Beaupré, S. Cho, N. Coates, J. S. Moon, D. Moses, M. Leclerc, K. Lee, A. J. Heeger, *Nat. Photonics*, 2009, **3**, 297; (d) G. Li, R. Zhu, Y. Yang, *Nat. Photonics*, 2012, **6**, 153; (e) L. Dou, J. You, J. Yang, C.-C. Chen, Y. He, S. Murase, T. Moriarty, K. Emery, G. Li, Y. Yang, *Nat. Photonics*, 2012, **6**, 180; (f) Y. Li, *Acc. Chem. Res.*, 2012, **45**, 723; (g) J. Chen, Y. Cao, *Acc. Chem. Res.*, 2009, **42**, 1709.
- (a) Z. He, C. Zhong, X. Huang, W.-Y. Wong, H. Wu, L. Chen, S. Su, Y. Cao, *Adv. Mater.* 2011, **23**, 4636; (b) Z. C. He, C. M. Zhong, S. J. Su, M. Xu, H. B. Wu, Y. Cao, *Nat. Photonics*, 2012, **6**, 591; (c) C. Gu, Y. C. Chen, Z. B. Zhang, S. F. Xue, S. H. Sun, K. Zhang, C. M. Zhong, H. H. Zhang, Y. Lv, F. H. Li, F. Huang, Y. G. Ma, *Adv. Energy Mater.*, 2014, DOI:10.1002/aenm.201301771. (d) L. Ye, S. Q. Zhang, W. C. Zhao, H. F. Yao, J. H. Hou, *Chem. Mater.*, 2014, **2**, 12484.
- (a) F. Huang, H. B. Wu, D. L. Wang, W. Yang, Y. Cao, *Chem. Mater.*, 2004, **16**, 708; (b) T. V. Pho, P. Zalar, A. Garcia, T.-Q. Nguyen, F. Wudl, *Chem. Commun.*, 2010, **46**, 8210; (c) J. F. Fang, B. H. Wallikewitz, F. Gao, G. L. Tu, C. Müller, G. Pace, R. H. Friend, W. T. S. Huck, *J. Am. Chem. Soc.*, 2011, **133**, 683.
- (a) J. H. Seo, A. Gutacker, B. Walker, S. Cho, A. Garcia, R. Q. Yang, T. Q. Nguyen, A. J. Heeger, G. C. Bazan, *J. Am. Chem. Soc.*, 2009, **131**, 18220; (b) L. Lan, J. Peng, M. Sun, J. Zhou, J. Wang, Y. Cao, *Org. Electron.*, 2009, **10**, 346.
- (a) Z. Tang, L. M. Andersson, Z. George, K. Vandewal, K. Tvingstedt, P. Heriksson, R. Kroon, M. R. Andersson, O. Inganäs, *Adv. Mater.*, 2012, **24**, 554; (b) S.-H. Oh, S.-I. Na, J. Jo, B. Lim, D. Vak, D.-Y. Kim, *Adv. Funct. Mater.*, 2010, **20**, 1977; (c) M. Lv, S. Li, J. J. Jasieniak, J. Hou, J. Zhu, Z. Tan, S. E. Watkins, Y. Li, X. Chen, *Adv. Mater.*, 2013, **25**, 6889; (d) S.-H. Liao, Y.-L. Li, T.-H. Jen, Y.-S. Cheng, S.-A. Chen, *J. Am. Chem. Soc.*, 2012, **134**, 14271; (e) S. Liu, K. Zhang, J. Lu, J. Zhang, H.-L. Yip, F. Huang, Y. Cao, *J. Am. Chem. Soc.*, 2013, **135**, 15326; (f) B. H. Lee, I. H. Jung, H. Y. Woo, H.-K. Shim, G. Kim, K. Lee, *Adv. Funct. Mater.*, 2014, **24**, 1100; (g) Y. Zhao, Z. Xie, C. Qin, Y. Qu, Y. Geng, L. Wang, *Solar Energy Materials & Solar Cells*, 2009, **93**, 604; (h) Q. Mei, C. H. Li, X. Gong, H. Lu, E. G. Jin, C. Du, Z. Lu, L. Jiang, X. Y., C. R. Wang, Z. S. Bo, *ACS Appl. Mater. Interfaces*, 2013, **5**, 8076; (i) S. Y. Yao, P. F. Li, J. Bian, Q. F. Dong, C. Imb, W. J. Tian, *J. Mater. Chem. A*, 2013, **1**, 11443; (j) J. H. Seo, A. Gutacker, Y. Sun, H. Wu, F. Huang, Y. Cao, U. Scherf, A. J. Heeger, G. C. Bazan, *J. Am. Chem. Soc.* 2011, **133**, 8416; (k) Y.-M. Chang, R. Zhu, E. Richard, C.-C. Chen, G. Li, Y. Yang, *Adv. Funct. Mater.*, 2012, **22**, 3284.
- (a) S. S. Li, M. Lei, M. L. Lv, S. E. Watkins, Z. A. Tan, J. Zhu, J. H. Hou, X. W. Chen, Y. F. Li, *Adv. Energy Mater.*, 2013, **3**, 1569. (b) X. Li, W. Zhang, Y. Wu, C. Mina, J. Fang, *J. Mater. Chem. A*, 2013, **1**, 12413; (c) C. Duan, C. Zhong, C. Liu, F. Huang, Y. Cao, *Chem. Mater.*, 2012, **24**, 1682; (d) C. Z. Li, C. C. Chueh, H. L. Yip, K. M. O'Malley, W. C. Chen, A. K. Y. Jen, *J. Mater. Chem. A*, 2012, **22**, 8574; (e) Z.-G. Zhang, B. Qi, Z. Jin, D. Chi, Z. Qi, Y. Li, J. Wang, *Energy Environ. Sci.*, 2014, **7**, 1966; (f) T. H. Reilly, A. W. Hains, H. -Y. Chen, B. A. Gregg, *Adv. Energy Mater.*, 2012, **2**, 455; (g) M. Vasilopoulou, D. G. Georgiadou, A. M. Douvas, A. Soulati, V. Constantoudis, D. Davazoglou, S. Gardelis, L. C. Palilis, M. Fakis, S. Kennou, T. Lazarides, A. G. Coutsolelos, P. Argitis, *J. Mater. Chem. A*, 2014, **2**, 182; (h) H. Ye, X. Hu, Z. Jiang, D. Chen, X. Liu, H. Nie, S. J. Su, X. Gong, Y. Cao, *J. Mater. Chem. A*, 2013, **1**, 3387; (i) K. Sun, B. Zhao, V. Murugesan, A. Kumar, K. Zeng, J. Subbiah, W. W. H. Wong, D. J. Jones, J. Ouyang, *J. Mater. Chem.*, 2012, **22**, 24155; (j) T. V. Pho, H. Kim, J. H. Seo, A. J. Heeger, F. Wudl, *Adv. Funct. Mater.*, 2011, **21**, 4338; (k) D. Chen, H. Zhou, M. Liu, W.-M. Zhao, S. J. Su, Y. Cao, *Macromol. Rapid Commun.*, 2013, **34**, 595; (l) C. H. Wu, C. Y. Chin, T. Y. Chen, S. N. Hsieh, C. H. Lee, T. F. Guo, A. K. Y. Jen, T.-C. Wen, *J. Mater. Chem. A*, 2013, **1**, 2582.
- X. Cheng, S. H. Sun, Y. C. Chen, Y. J. Gao, L. Ai, T. Jia, F. H. Li, Y. Wang, *J. Mater. Chem. A*, 2014, **2**, 12484.
- H. Zhou, Y. Zhang, J. Seifert, S. D. Collins, C. Luo, G. C. Bazan, T.-Q. Nguyen, A. J. Heeger, *Adv. Mater.*, 2013, **25**, 1646.
- E. Zimmermann, P. Ehrenreich, T. Pfadler, J. A. Dorman, J. Weickert, L. Schmidt-Mende, *Nat. Photonics*, 2014, **8**, 669.
- (a) C. J. Van Oss, L. Ju, M. K. Chaudhury, R. J. Good, *J. Colloid Interface Sci.*, 1989, **128**, 313; (b) C. J. Van Oss, M. K. Chaudhury, R. J. Good, *Chem. Rev.* 1988, **88**, 927; (c) K. X. Ma, T. S. Chung, R. J. Good, *J. Polym. Sci., Part B: Polym. Phys.*, 1998, **36**, 2327; (d) X. J. Wang, T. Ederth, O. Inganäs, *Langmuir*, 2006, **22**, 9287.
- D. Ma, M. L. Lv, M. Lei, J. Zhu, H. Q. Wang, X. W. Chen, *ACS Nano.*, 2014, **8**, 1601.
- J. P. Fox, D. P. Goldberg, *Inorg. Chem.* 2003, **42**, 8181.

A table of contents



$\text{ZnPc}(\text{OC}_8\text{H}_{17}\text{OPyCH}_3\text{I})_8$ with good adhesion to active layer has been utilized as a cathode interlayer for highly efficient polymer solar cells.